Quantum-Classical Correspondence through Entanglement Dynamics

Lock Yue Chew[1] and Ning Ning Chung[2]

[1] Nanyang Technological University, 21 Nanyang Link, SPMS-PAP-04-04,
   Singapore 637371
   (E-mail: `lockyue@ntu.edu.sg`)
[2] Temasek Laboratory, National University of Singapore, Singapore 117508
   (E-mail: `tslcnn@nus.edu.sg`)

Abstract. In the study of quantum chaos relating to entanglement dynamics, it is found that local dynamical features in the classical phase space, such as the tori in regular island and the chaotic sea, can have subtle influence on the entanglement production rate, the maximum entanglement entropy etc. In this paper, we revisit the two-coupled quartic oscillator system, whose entanglement dynamics was shown by Chung and Chew (2009, *Phys. Rev. E*, **80** 016204) to be insensitive to these local dynamical features. By means of a comprehensive set of initial coherent states, and by considering both the quantum and semi-classical regime, we provide additional numerical evidence and physical insights that support the conclusion that the entanglement dynamics of this system is dependent on the global classical dynamical regime while insensitive to the local classical behavior.
Keywords: Quantum-classical correspondence, Entanglement dynamics, Quantum chaos, Classical chaos, Coupled quartic oscillators, Quantum information processing.

1 Introduction

The problem of quantum-classical correspondence is related to the subject of quantum chaos. The study of how a classically chaotic system has a mysterious influence on its quantized counterpart has made quantum chaos a fasinating subject. The influence of chaos, instead of leading to an exponential divergence of quantum wavefunctions through minute changes of initial conditions (which is not possible since Schrödinger equation is linear), left its imprint through quantum properties such as the energy level statistics, the localization, or the scarring of the wavefunction [1].

Recently, there is great interest in the study of the effect of classical chaos on the entanglement between composite quantum system [2–7]. This results from the fact that entanglement is an important resource for information processing in the quantum regime. In particular, its non-classical feature has enabled the creation of novel information processing paradigms. For example, entanglement has important application in superdense coding, quantum teleportation

and quantum cryptography [8]. The importance of entanglement for quantum information processing suggests the need to generate entangled quantum states. A particular approach to create entangled quantum states is by means of quantum harmonic and anharmonic oscillator systems. Experimentally, quantum harmonic oscillator system has been achieved in the form of a micromechanical resonators strongly coupled to an optical field [9]. An extension to this system has also been proposed with the resonator interact with a trapped atom through a quantized light field in a laser driven high-finesse cavity [10]. On the other hand, quantum anharmonic oscillator system can be implemented by optical fibre with Kerr nonlinearities. By injecting coherent states into such a fibre, two Schrödinger cat-like states can be generated [11].

The consideration of the effects of chaos on entanglement have led to the studies of many diverse systems beyond quantum anharmonic oscillator systems. These systems are coupled kicked tops [2,7], Rydberg molecules [5] and interacting spin systems [6]. Generically, it is found in these investigations that when the classical system is more chaotic, the corresponding quantized system has more entanglement and also a faster entanglement production rate, although there are some notable exceptions [12,13]. In addition, the frequency of oscillation of the entanglement dynamics increases as the classical system becomes more chaotic. An important observation made by many researchers [4,5,2] is that the magnitude and production rate of the entanglement is dependent on the local dynamical structure of the corresponding classical phase space. This places the existence of a universal quantum-classical correspondence in terms of dynamcial entanglement production in a doubtful position. However, we have shown in [3] that contrary to such a local phase space dependence, it is possible for the entanglement dynamics to depend solely on the global classical dynamical regime.

In this paper, we will present our investigation on the correspondence between classical system and its quantized version through the entanglement entropy. More precisely, for the classical systems, we shall study its dynamics in the classical phase space and then relate it to the corresponding entanglement dynamics in the quantized system. We shall study such quantum-classical correspondence in an anharmonic oscillator system that can exhibit regular, mixed and purely chaotic dynamics. By perfoming detailed numerical computations, we have strengthed our earlier conclusion in [3] that it is possible for the entanglement dynamics to depend on the global classical dynamical regime.

2   The Coupled Quartic Oscillator

To begin, let us introduce our coupled nonlinear oscillator system. It is the coupled quartic oscillator given by the following Hamiltonian [14]:

$$H = \frac{1}{2}\left(p_1^2 + p_2^2\right) + 3x_1^4 + x_2^4 - \lambda x_1^2 x_2^2,\tag{1}$$

where p_1 and p_2 are the momenta, x_1 and x_2 the positions of the oscillator, and λ is the coupling constant. Depending on the value of λ, the classical dynamics

of this coupled quartic oscillator can display three distinct features: (a) regular dynamics (see Fig. 1), (b) a mixture of regular and chaotic dynamics (see Fig. 2), and (c) purely chaotic dynamics (see Fig. 3). Note that Figs. 1 to 3 gives the Poincaré section of the dynamics in the x_2-p_2 plane with $x_1 = 0$ and $p_1 > 0$.
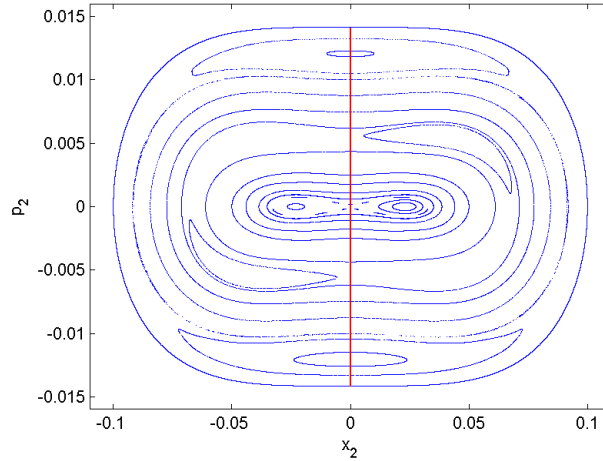

Fig. 1. Classical phase portrait for the coupled quartic oscillator system with coupling constant $\lambda = 0.4$. Note that twenty-nine equally spaced points are selected on the straight line with their corresponding coherent states serve as initial conditions for the entanglement dynamics evaluation.

Next, we proceed to quantize the coupled quartic oscillator system and investigate its quantum dynamics. This requires us to replace x_i and p_i with the corresponding operators $\hat{x}_i$ and $\hat{p}_i$. We select the product states $|n_1\rangle \otimes |n_2\rangle$ as our basis for the numerical computation. $|n_1\rangle$ and $|n_2\rangle$ are the eigenvectors of the harmonic oscillator. With this basis, we can express the Schrödinger equation in the following form:

$$i\hbar \frac{d}{dt}\langle m_1 m_2|\psi(t)\rangle = \sum_{n_1=0}^{M}\sum_{n_2=0}^{M}\langle m_1, m_2|\hat{H}|n_1, n_2\rangle\langle n_1, n_2|\psi(t)\rangle, \qquad (2)$$

where $\hat{H}$ is the quantized Hamiltonian and $|\psi(t)\rangle$ the quantum state at time t of the two-coupled quartic oscillator. For the sake of computation, we have truncated the size of the basis to M. Thus, $\langle m_1, m_2|\hat{H}|n_1, n_2\rangle$ is a four-dimensional matrix. The initial states $|\psi(0)\rangle$ are chosen to be the coherent states $|\alpha_1\rangle \otimes |\alpha_2\rangle$, which provides the connection between the classical and quantum domains. More specifically, the center of the coherent state corresponds precisely to the point (x_1, p_1, x_2, p_2) in the classical phase space, with $\alpha_l = (x_l + ip_l)/\sqrt{2}$. With the defined initial quantum state, we evolve the states of the bipartite quantum system numerically through Eq. (2). Note that more efficient com-
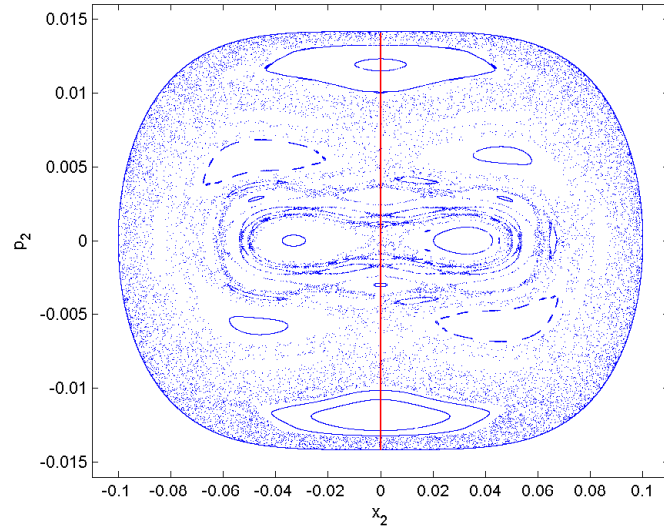
Fig. 2. Classical phase portrait for the coupled quartic oscillator system with coupling constant $\lambda = 0.8$. Note that twenty-nine equally spaced points are selected on the straight line with their corresponding coherent states serve as initial conditions for the entanglement dynamics evaluation.
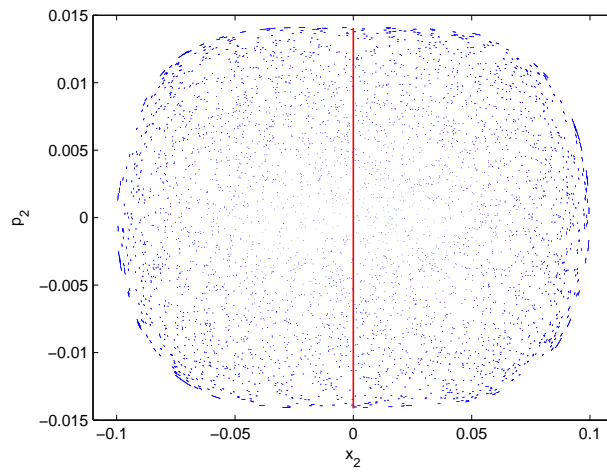

Fig. 3. Classical phase portrait for the coupled quartic oscillator system with coupling constant $\lambda = 2.7$. Note that twenty-nine equally spaced points are selected on the straight line with their corresponding coherent states serve as initial conditions for the entanglement dynamics evaluation.

putation can be achieved with the two-step approach [15–17] since it is suited for the evaluation of the time-evolved states of nonlinear quantum systems.

The entanglement dynamics is determined through the time variation of the von Neumann entropy, which is defined as follow:

$$S_{VN}(t) = -\text{Tr}\left(\rho_1(t)\ln\rho_1(t)\right),\tag{3}$$

where

$$\rho_1(t) = \text{Tr}_2\left(\rho(t)\right)\tag{4}$$

is the reduced density matrix of oscillator 1. It is obtained by taking the partial trace over oscillator 2 on the density matrix $\rho(t)$ of the two-coupled quantum quartic oscillator, as shown in Eq. (4). Note that since

$$\rho(t) = |\psi(t)\rangle\langle\psi(t)|$$

is pure as our system is assumed to be protected from the decohering environment, the von Neumann entropy is an applicable measure of quantum entanglement. Furthermore, the replacement of $\rho_1(t)$ by the reduced density matrix of oscillator 2,

$$\rho_2(t) = \text{Tr}_1\left(\rho(t)\right),$$

in Eq. (3) would not make any difference to the evaluation of the entanglement entropy.

In [3], we had computed the entanglement dynamics by picking coherent states which correspond to points in the classical phase space for each of the dynamical regimes, i.e., the regular, the mixed and the chaotic regimes (refer to Figs. 3 to 5 in [3]). For example, a selection of points in the mixed phase space with some in the regular islands and some in the chaotic sea had been picked (see Fig. 4 of [3]) with the corresponding coherent states serve as initial points for the entanglement dynamics calculation.

We had performed this computation in the quantum and semi-classical regimes. We had employed the parameter $R = \hbar/\Lambda$ to quantify the "quantumness" of the system. Note that $\Lambda = |\alpha_1|^2 + |\alpha_2|^2$ is the action of the system with α_1 and α_2 being the coordinates of the coherent state. When $R \gg 1$, the system is in the quantum regime. On the contrary, when $R \ll 1$, the system is in the semi-classical regime. The semi-classical regime can be approached in either of two ways: $\hbar \to 0$ or $\Lambda \to \infty$. The latter case in fact corresponds to the high-energy approximation in the semi-classical theory. The former case is the one adopted in this paper.

Our earlier results [3] show that the entanglement entropy is much larger in the semi-classical regime. We observe that for both the quantum and semi-classical regimes, the entanglement production is the highest in the pure chaos case, follow by the mixed case, and is lowest in the regular case. We also observe that when the classical system becomes more chaotic, the frequency of oscillation of the entanglement dynamics increases. These results correspond to those reported in the literature. However, for each of the regular, mixed and chaotic case, we observe that identical results are obtained when different initial conditions are employed. This is a surprising result that differs from others

in the literature. This result has led us to conclude in [3] that it is possible for
the entanglement dynamics to depend entirely on the global dynamical regime
while insensitive to the local classical behavior.

3   Results and Discussion

One may question the conclusion at the end of the last section as follow: is
it possible that such global dependence arises from the choice of the initial
coherent states? This query is especially relevant for the mixed case as the
chosen initial coherent states may lie too close to the edge of the regular island,
thus allowing it to sample the chaotic sea surrounding the island. This may
have obscured the local dynamical structure and led to the identical results
observed.

In this section, we present numerical results that will address these issues.
To do this, we need to check the conclusion with a more extensive choice of
initial conditions. In consequence, we select a set of initial conditions that lie
along the straight lines as shown in Figs. 1, 2 and 3 for the regular, mixed and
chaotic case respectively. By considering twenty-nine initial conditions that are
equally and closely spaced on each of these straight lines, we can ascertain the
validity of the conclusion since these initial conditions correspond to different
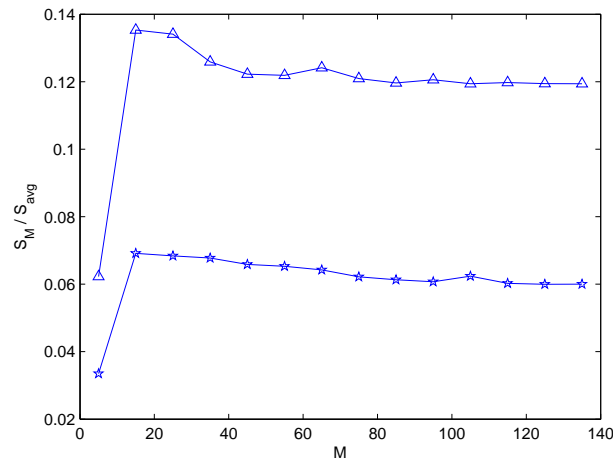local dynamical features of the classical phase space.

Fig. 4. The maximum and average entanglement entropy versus the basis size M.
Note that the computation is based on $\lambda = 0.8$.

Due to the existence of scale invariance in the classical dynamics of Eq.
(1) [14], we can select an energy $E = 0.0001$ that is small so that we do not
need to use a large basis size for our numerical calculation of the entanglement
dynamics. Our computations, as illustrated in Fig. 4, shows that a size of

$M = 135$ is sufficient to ensure convergence for our calculation. With this basis size, we determine the maximum entanglement entropy

$$S_M = \max_t S_{VN}(t)$$

and the mean entanglement entropy

$$S_{avg} = \frac{1}{T} \int_0^T S_{VN}(t)dt$$

of the entanglement dynamics, which are initiated by coherent states that correspond to the set of initial conditions discussed above. In our computation, we consider $\hbar = 1$ for the quantum regime and $\hbar = 0.00001$ for the semi-classical regime. This implies an uncertainty circle with size of order 0.7 for the quantum regime and 0.002 for the semi-classical regime.
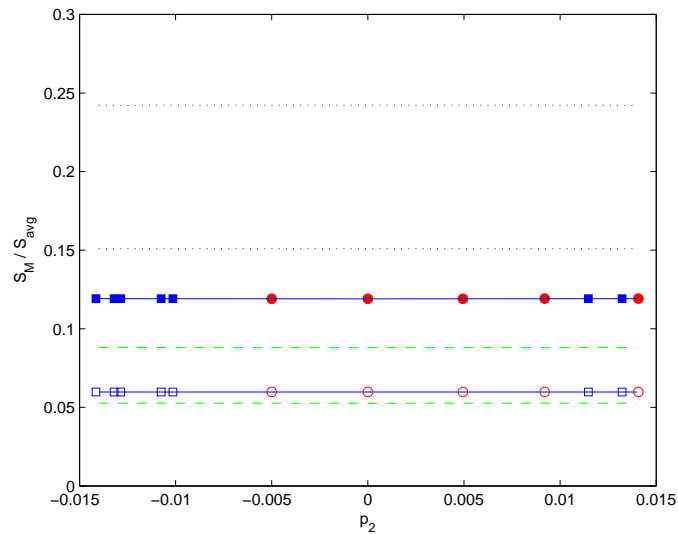

Fig. 5. The maximum and average entanglement entropy for initial coherent state in the quantum regime with $x_1 = x_2 = 0$ but different values of p_1 and p_2. From top to bottom, we have S_M and S_{avg} for $\lambda = 2.7$, S_M for $\lambda = 0.8$ and 0.4, S_{avg} for $\lambda = 0.8$ and 0.4. Note that the parameters used are $\hbar = 1$, $M = 135$ and $E = 0.0001$. Note that the circles and squares represent a sample of the chaotic and regular initial conditions respectively.

Our results for the regular case (dashed lines in Figs. 5 and 6) show a constant S_M and S_{avg} for all the initial coherent states in both the quantum and semi-classical regime. This is in marked contrast to [4] where initial coherent states that situate on the outer tori have a larger entanglement entropy than those that locate at the inner tori. Interestingly, the outcome here for a
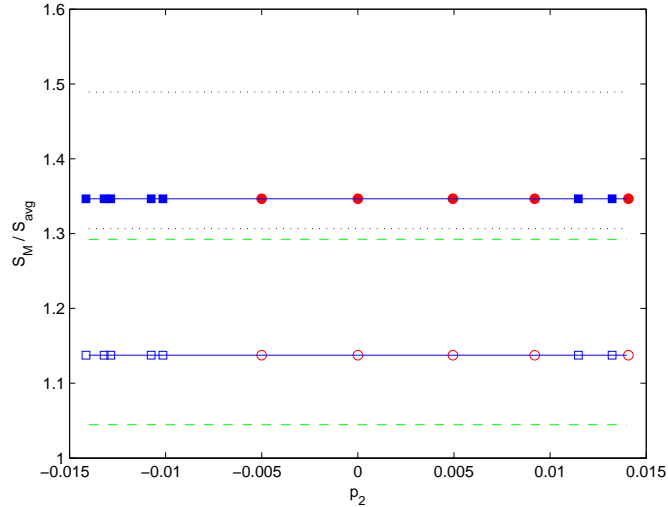
Fig. 6. The maximum and average entanglement entropy for initial coherent state in the semi-classical regime with $x_1 = x_2 = 0$ but different values of p_1 and p_2. From top to bottom, we have S_M for $\lambda = 2.7$ and 0.8, S_{avg} for $\lambda = 2.7$, S_M for $\lambda = 0.4$, S_{avg} for $\lambda = 0.8$ and 0.4. Note that the parameters used are $\hbar = 0.00001$, $M = 135$ and $E = 0.0001$. Note that the circles and squares represent a sample of the chaotic and regular initial conditions respectively.

nonlinear oscillator system is analogous to that of the linear systems discussed in [3].

In addition, Figs. 5 and 6 also show that S_M and S_{avg} attain a constant value for all the chosen initial coherent states in the mixed case (solid lines in the figures). This may be explained by the fact that the uncertainty circle of the initial coherent states in the quantum regime is large enough to sample a mixture of different local phase space structures, leading to the uniform results. However, with similar results obtained in the semi-classical regime, this explanation becomes untenable since the uncertainty circle of the initial coherent states is sufficiently small in this case for the differentiation of local phase space structure.

Finally, we observe a constant S_M and S_{avg} for the chaotic case as shown by the dotted lines in Figs. 5 and 6.

4   Conclusions

By means of a more comprehensive range of initial coherent states that correspond to diverse local dynamical structures in the classical phase space, we have shown that S_M and S_{avg} are insensitive to the choice of the initial coherent states. This is shown to be true for the regular, mixed and chaotic cases in both the quantum and semi-classical regimes for the coupled quartic oscillator

system. We have thus reaffirmed our earlier conclusion that it is possible for the entanglement dynamics to depend solely on the global classical dynamical regime while insensitive to the local classical behavior. An advantage of models that possess such global dependence is that they can serve to generate encoding subspaces that are stable against any errors in the preparation of the initial separable coherent states. We believe that these encoding subspaces will be significant in the design of robust quantum information processing protocol.

References

1. G. Casati and B. Chirikov. Quantum chaos: between order and disorder. Cambridge University Press, 1995.
2. M. Lombardi and A. Matzkin. Entanglement and chaos in the kicked top, Physical Review E, vol. 83, 016207, 2011.
3. N. N. Chung and L. Y. Chew. Dependence of entanglement dynamics on the global classical dynamical regime, Physical Review E, vol. 80, 016204, 2009.
4. S. Zhang and Q. Jie. Quantum-classical correspondence in entanglement production: entropy and classical tori, Physical Review A, vol. 77, 012312, 2008.
5. M. Lombardi and A. Matzkin. Scattering-induced dynamical entanglement and the quantum-classical correspondence, Europhysics Letters, vol. 74, 771-777, 2006.
6. M. Novaes. Entanglement dynamics for two interacting spins, Annals of Physics, vol. 318, 308-315, 2005.
7. P. A. Miller and S. Sarkar. Signatures of chaos in the entanglement of two coupled quantum kicked tops. Physical Review E, vol. 60, 1542-1550, 1999.
8. J. Audretsch, Entangled systems: new directions in quantum physics, Wiley-VCH, 2007.
9. S. Gröblacher, K. Hammerer, M. R. Vanner and M. Aspelmeyer. Observation of strong coupling between a micromechanical resonator and an optical cavity field, Nature, vol. 460, 724-727, 2009.
10. K. Hammerer, M. Wallquist, C. Genes, M. Ludwig, F. Marquardt, P. Treutlein, P. Zoller, J. Ye and H. J. Kimble. Strong coupling of a mechanical oscillator and a single atom, Physical Review Letters, vol. 103, 063005, 2009.
11. B. Yurke and D. Stoler. Generating quantum mechanical superpositions of macroscopically distinguishable states via amplitude dispersion, Physical Review Letters, vol. 57, 13-16, 1986.
12. H. Fujisaki, T. Miyadera and A. Tanaka. Dynamical aspects of quantum entanglement for weakly coupled kicked tops, Physical Review E, vol. 67, 066201, 2003.
13. M. Novaes and M. A. M. De Aguiar. Entanglement and chaos in a square billiard with a magnetic field, Physical Review E, vol. 70, 045201(R), 2004.
14. M. Tomiya, N. Yoshinaga, S. Sakamoto and A. Hirai. A large number of higher-energy eigenvalues of a huge dimensional matrix for a quantum chaotic study of a quartic potential, Computer Physics Communications, vol 169, 313-316, 2005.
15. N. N. Chung and L. Y. Chew. Two-step approach to the dynamics of coupled anharmonic oscillators, Physical Review A, vol. 80, 012103, 2009.
16. N. N. Chung and L. Y. Chew. Energy eigenvalues and squeezing properties of general systems of coupled quantum anharmonic oscillators, Physical Review A, vol. 76, 032113, 2007.
17. C. S. Hsue and J. L. Chern. Two-step approach to one-dimensional anharmonic oscillators, Physical Review D, vol. 29, 643-647, 1984.